CHIN.PHYS.LETT. Vol. 18, No. 3 (2001) 361

Many-Body Potentials for Intermetallic TiAl Alloy and Its Point Defect Properties *

WANG Tian-Min(王天民)[1], WANG Bao-Yi(王宝义)[2], JU Xin(巨新)[2], GU Qiang(顾强)[3], WANG Yue-Xia (王月霞)[3], GAO Fei (高飞)[3]

[1] *The School of Science, Beijing University of Aeronautics and Astronautics, Beijing 100083*
[2] *Institute of High Energy Physics, Chinese Academy of Sciences, Beijing 100039*
[3] *Department of Materials Science, Lanzhou University, Lanzhou 730000*

(Received 10 June 2000)

For the intermetallic compound TiAl, the interatomic potentials in the Finnis–Sinclair model were constructed by empirically fitting to the properties of $L1_0$ TiAl tetragonal phase and the pressure–volume relations. In the calculations of the point defect properties of the TiAl alloy with this potential, it was shown that the thermal concentration of anti-site defects was higher than that of other point defects. With similar formation energies, five possible interstitial configurations were stable. This model was consistent with the embedded atom method or embedded defect method and adequate for simulation of defects in the TiAl alloy.

PACS: 34. 20. Cf, 61. 72. Ji

Ti–Al base alloys are excellent candidate materials in the aerospace industry for their low density and attractive high-temperature properties.[1] To investigate the microstructures, the properties of alloys in atomic scale, such as structures of dislocations, grain boundaries and configuration of point defects, are important in understanding the alloy behaviour.[1] Molecular dynamics simulation is a powerful method for investigating point defect properties and the mechanism of defect diffusion.[2] The study of interatomic potentials has made a significant advancement since the introduction of the embedded atom method (EAM)[3] and Finnis–Sinclair (F–S) many-body potentials.[4] Both of the models add a similar many-body item to a pairwise potential and such modifications make the description of atomic potentials in metals and alloys more accurate than a pairwise potential. Ackland *et al.*[5] improved the F–S model to describe interatomic forces in an alloy. In this letter, the F–S many-body potentials for the intermetallic compound TiAl are reported and the properties of point defects in the TiAl alloy are simulated by the molecular dynamic method.

For a binary alloy system of atom species of A and B, the energy of an assembly of N atoms in the F–S model modified by Ackland *et al.*[5] is expressed as

$$E = \sum_i^N \Big(\frac{1}{2} \sum_{j \neq i}^N V(R_{ij}) - \sqrt{\rho_i} \Big),$$
$$\rho_i = \sum_{j=1}^N \Phi(R_{ij}), \qquad (1)$$

where i and j refer to individual atoms. V is a repulsive core–core interaction and the many-body term represents the band energy, Φ is regarded as a sum of the squares of overlap integrals within the tight-binding approach. Both V and Φ are empirically fitted potentials in which R_{ij} is the distance between the ith and jth atoms.

There are six pair potentials $V_{\rm AA}$, $V_{\rm BB}$, $V_{\rm AB}$, $\Phi_{\rm AA}$, $\Phi_{\rm BB}$ and $\Phi_{\rm AB}$ for a binary alloy. $V_{\rm AA}$, $V_{\rm BB}$, $\Phi_{\rm AA}$ and $\Phi_{\rm BB}$ are assumed to be independent of the concentration of the alloy and can be treated the same as those in pure metals. The potential parameters for pure metals have been fitted to reproduce the equilibrium lattice parameter, cohesive energy, elastic moduli, vacancy formation energy and stacking fault energy. The parameters, defined as a_k^{AA} $(k = 1, 6)$ and A_k^{AA} $(k = 1, 2)$ in which a_6^{AA} was fitted from $P - V$ relation[6] for Ti and Al, are summarized in Table 1 from Refs. [6, 7]. With the interpretation of hopping integrals, Φ_{AB} is considered as the geometrical mean of Φ_{AA} and Φ_{BB}. Only V_{AB} was fitted to alloy properties with a cubic spline form as follows[5,7]

$$V_{AA}(R_{ij}) = \sum_{k=1}^{6} a_k^{AA} H(r_k^{AA} - R_{ij})(r_k^{AA} - R_{ij})^3,$$
$$\Phi_{AA}(R_{ij}) = \sum_{k=1}^{2} A_k^{AA} H(R_k^{AA} - R_{ij})(R_k^{AA} - R_{ij})^3,$$
$$V_{AB}(R_{ij}) = \sum_{k=1}^{3} a_k^{AB} H(r_k^{AB} - R_{ij})(r_k^{AB} - R_{ij})^3,$$
$$\Phi_{AB}(R_{ij}) = \sqrt{\Phi_{AA}(R_{ij})\Phi_{BB}(R_{ij})}, \qquad (2)$$

where $H(x)$ is the Heaviside unit-step function which gives the cut-off distance of each spline segment. V_{BB} and Φ_{BB} have the same form as V_{AA} and Φ_{AA}.

By fitting the equilibrium state parameters of the cohesive energy and lattice parameters,[8] three of $a_k^{\rm TiAl}$ $(k = 1, 2, 3)$ for $V_{\rm TiAl}$ could be obtained by the following conditions,

$$E_{\rm coh} = \Delta H^{\rm mix} + \frac{1}{2} E_{\rm coh}^{\rm Ti} + \frac{1}{2} E_{\rm coh}^{\rm Al}$$
$$\frac{\partial E^{\rm alloy}}{\partial a} = 0$$
$$\frac{\partial E^{\rm alloy}}{\partial c} = 0 \qquad (3)$$

*Supported by the National Natural Science Foundation of China under Grant No. 59895150.
©2001 Chinese Physical Society and IOP Publishing Ltd

where $E_{\rm coh}^{\rm Ti}$ and $E_{\rm coh}^{\rm Al}$ are the cohesive energies of Ti and Al, respectively. $\Delta H^{\rm mix}$ is the enthalpy of mixing[9] and $r_k^{\rm TiAl}$ are chosen as knot points such that $r_1^{\rm TiAl} > r_2^{\rm TiAl} > r_3^{\rm TiAl}$ and $r_1^{\rm TiAl}$ represents the cut-off radius of $V_{\rm TiAl}$.

Table 1. Parameters for many-body potentials of Ti–Ti, Al–Al and Ti–Al, used here for $L1_0$ TiAl.

	Ti–Ti	Al–Al	Ti–Al
a_1	−57.0991	32.2388	−0.05685
a_2	80.7356	−74.561	0.128061
a_3	−21.7615	140.0125	5.791351
a_4	−10.3965	−107.579	−2.45
a_5	74.51503	29.4447	
a_6	35.92102	101.55	
A_1	39.79593	19.2224	
A_2	−40.0613	4.9595	
r_1	1.22	1.225	5.44975
r_2	1.2	1.18	4.99895
r_3	1.12	1.09	2.95225
r_4	0.95	1.05	2.8
r_5	0.8	0.9	
r_6	0.707	0.707	
R_1	1.22	1.2	
R_2	1.05	0.93	
a (nm)	0.4173	0.405	0.399, 0.408

The potential parameters mentioned above are derived from the equilibrium state of TiAl. Therefore, they are only suitable for calculating the interactions when the atomic space is equal to, or larger than the equilibrium nearest-neighbour distance. Simulating the properties in which the atoms are forced close together, such as the compressibility at high pressure and self-interstitial properties, the potentials need to be modified. By comparing the pressure–volume ($P-V$) relation with the experimental data, the fourth item for $V_{\rm TiAl}$ can be obtained.

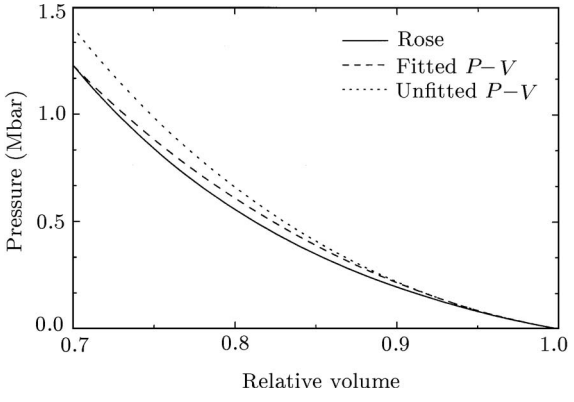

Fig. 1. Pressure–volume relation for TiAl.

Because the experimental data for TiAl are not available to us, we have to turn to the empirical relation provided by Rose *et al.*[10] When we know the equilibrium lattice constants a and c, cohesive energy $E_{\rm coh}$ and bulk modulus B, the $P-V$ relation of Rose can be determined. The data for TiAl are listed in Table 2 in which the bulk modulus B is acquired from the following formula,[11]

$$B = \frac{(C_{11}+C_{12})C_{33} - 2C_{13}^2}{C_{11}+C_{12}+2C_{33}-4C_{13}}. \qquad (4)$$

Figure 1 shows the $P-V$ curves calculated from both the potential and the Rose model. We see that, with adding a fourth item, the $P-V$ curve becomes consistent to the Rose model.

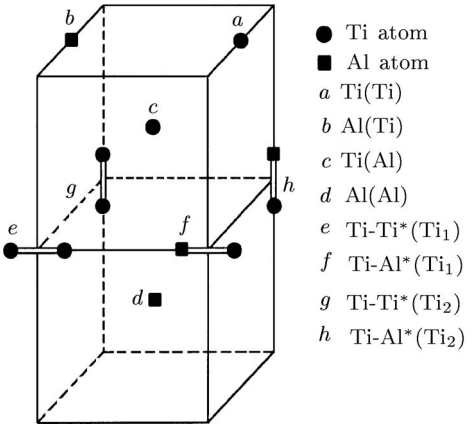

Fig. 2. Four octahedral interstitials and the dumb-bell interstitials at Ti atom sites in TiAl (the dumb-bell interstitials at Al atom sites are similar and are not given).

Table 2. Parameters of TiAl for fitting the $P-V$ relation.

Properties	Values	References
B (10^{11} Pa)	1.4	This work
$E_{\rm coh}$(eV)	4.519	[9]
a (nm)	0.3999	[8]
c (nm)	0.4080	[8]

Table 3. Parameters for $L1_0$ TiAl.

Properties	Experimental or first principle[12]	EDM[12]	EAM[12]	This work
a (0.1 nm)	3.999	3.95	3.95	3.999
c (0.1 nm)	4.080	4.14	4.14	4.080
$E_{\rm c}$ (eV)	4.519	4.39	4.39	4.52
C_{11} (eVÅ^{-3})	1.19	1.18	1.28	1.208
C_{12} (eVÅ^{-3})	0.65	0.53	0.58	0.48
C_{13} (eVÅ^{-3})	0.56	0.65	0.96	0.856
C_{33} (eVÅ^{-3})	2.09	1.69	1.15	1.593
C_{44} (eVÅ^{-3})	0.75	0.89	0.86	0.675
C_{66} (eVÅ^{-3})	0.31	0.5	0.47	0.301

Table 4. Point defect properties of TiAl. Here α, β and γ represent the stable configurations of Al(Al)[110], Ti(Ti)[110] and Al-Al*(Al_1), respectively. The symbol # denotes that the defect configuration is not stable, and the relaxed configuration is shown in the column of $E_{\rm d}^{\rm f}$.

Defect	$E_{\rm d}^{\rm f}$ (eV)	$V_{\rm d}/V_0$	Defect	$E_{\rm d}^{\rm f}$ (eV)	$V_{\rm d}/V_0$
Vacancy			Dumb-bell		
$V_{\rm Al}$	0.99	0.8	Al–Al*(Al_1)	3.8	2.46
$V_{\rm Ti}$	1.71	0.8	Al–Ti*(Al_1)	$Ti_{Al}+\gamma$	#
Anti-site			Al–Al*(Al_2)	5.98	2.87
Al_{Ti}	0.89	1	Al–Ti*(Al_2)	β	#
Ti_{Al}	−0.74	1	Ti–Al*(Ti_1)	$Al_{Ti}+\beta$	#
Crowdion			Ti–Ti*(Ti_1)	β	#
Al(Al)[110]	3.66	2.46	Ti–Al*(Ti_2)	α	#
Ti(Al)[110]	$Ti_{Al}+\alpha$	#	Ti–Ti*(Ti_2)	3.95	2.87
Ti(Ti)[110]	3.88	2.66	Octahedral		
Al(Ti)[110]	$Al_{Ti}+\beta$	#	Al(Al)	$Ti_{Al}+\alpha$	#
Al[011]	γ	#	Ti(Al)	β	#
Ti[011]	$Ti_{Al}+\gamma$	#	Al(Ti)	α	#
			Ti(Ti)	$Al_{Ti}+\beta$	#

With the F–S potentials of the TiAl alloy, the calculated elastic constants are in good agreement with

the experimental ones, as shown in Table 3. There are two Cauchy pressures $(C_{12}-C_{66})$ and $(C_{13}-C_{44})$ in the $L1_0$ structure of TiAl; one of them is positive and the other is negative. However, neither the result of the F–S potentials nor the EAM model[12] can account for this fact. Adding an angular-dependent item in EAM, the EDM[12] gives the right relationship for the two Cauchy pressures. It is necessary to point out that, for the $L1_0$ TiAl alloy, the EAM or EDM result in poor values for some elemental parameters, such as the lattice constants and cohesive energy.

With the current potential, the formation energies and formation volumes for some configurations of the point defect in TiAl alloy were calculated by molecular dynamics. A program, developed by Gao,[6] was modified to be suitable for the $L1_0$ structure and used for the calculation with periodic boundary conditions and constant pressure (0 Pa) relaxation at a temperature of 0 K.

There are two kinds of vacancies and two anti-site defects in a TiAl alloy. The configurations of self-interstitial atoms are much more complex. The two types of octahedral sites, located on the Ti atom plane and the Al atom plane, respectively, lead to four possible interstitial configurations of Ti(Ti), Al(Ti) (on the Ti atom plane) and Ti(Al), Al(Al) (on the Al atom plane). Moreover, eight possible $\langle 100\rangle$ dumbbell configurations, $A-B^*(\mathrm{A}_1)$, (lying on the A atom plane) and $A-B^*(A_2)$, (vertical to the A atom plane) as demonstrated in Fig. 2, and six crowdions in close-packed directions are discussed. Here, A and B represent a Ti atom or an Al atom and the asterisk denotes the interstitial atom.

The definition of formation energy $E_{\mathrm{d}}^{\mathrm{f}}$, is given in Eq. (5).[6] The formation volumes for vacancies, $V_{\mathrm{d}}^{\mathrm{Vac}}$, were obtained by adding the volume V_0 per atom in perfect TiAl to the relaxation volume computed in simulations. $V_{\mathrm{d}}^{\mathrm{Int}}$ and $V_{\mathrm{d}}^{\mathrm{Ant}}$, for interstitials and anti-site defects, were simply the relaxation volumes.[6]

$$E_{\mathrm{d}}^{\mathrm{f}} = E_{\mathrm{Block}} - N_{\mathrm{Ti}}\mu_{\mathrm{Ti}} - N_{\mathrm{Al}}\mu_{\mathrm{Al}}, \qquad (5)$$

where E_{Block} is the total energy of the crystal with defects, N_{Ti} and μ_{Ti} are the number and chemical potential of the Ti atom in the crystal. The formation energy and volume for each of the point defects are presented in Table 4.

The vacancy formation energy on the Al sublattice, $E_{\mathrm{Al}}^{\mathrm{f}} = 0.99$ eV, is much lower than that on the Ti sublattice, $E_{\mathrm{Ti}}^{\mathrm{f}} = 1.71$ eV. Basically the same results, $E_{\mathrm{Al}}^{\mathrm{f}} = 1.02$ eV, $E_{\mathrm{Ti}}^{\mathrm{f}} = 1.30$ eV were obtained by the EAM.[12] Experimentally, if the vacancy formation energy is much lower on one sublattice, this value should be observed because the vacancy formation on this sublattice would be dominant. However, the thermal vacancy formation enthalpy, $H_{\mathrm{V}}^{\mathrm{f}} = 1.4 \pm 0.06$ eV, in the TiAl alloy was determined by Brossmans *et al.*[13] Farkas[12] added an angular-dependent term in his EAM model and obtained the values of 1.24 eV for $E_{\mathrm{Al}}^{\mathrm{f}}$ and of 1.49 eV for $E_{\mathrm{Ti}}^{\mathrm{f}}$, which are closer to the experimental values. The formation energies of anti-sites are lower than those of vacancies and self-interstitials. Therefore, we expect that the thermal concentration of anti-site defects should be higher than that of the other point defects. By fitting the experimental data to the nearest-neighbour bond models, the same conclusion is reached.[13]

As far as we know, the properties of the interstitial in TiAl have not been reported. Based on the results of this work, we concluded from Table 4, that most interstitial configurations are not stable and transform spontaneously to other stable configurations during the relaxation. The formation energies of the stable interstitial configurations are two to three times greater than for vacancies. It is interesting to observe that, with respect to the formation of crowdions, all the four possible octahedral configurations are unstable and transform to other configurations. The Al(Al)[110] crowdion, with the lowest formation energy, is energetically favoured in the five stable interstitial configurations. The differences in formation energies of Al(Al)[110], Ti(Ti)[110], Al–Al*(Al1) and Ti–Ti*(Ti_2) configurations are small and typically, in the range of 0.2 to 0.3 eV, implying nearly equal opportunities for the formation of Ti and Al interstitials.

As the radii of the Ti and Al atom are very close, the calculated formation volumes for the Ti defect are close to those of Al. The results also show that the formation volumes of the interstitial are much larger than other point defects. For the same kind of interstitial atoms, generally, the greater the formation volume is, the larger the formation energy will be.

In summary, the many-body potential in the F–S model was constructed and used to describe the atomic interactions in $L1_0$ TiAl alloys. The calculations showed that the thermal concentration of anti-site defects was higher than that of other point defects. Only five possible interstitial configurations were stable. This model was consistent to the EAM or EDM models and suitable for simulating the elastic properties and point defects by molecular dynamics.

References

[1] Panova J and Farkas D 1998 *Phil. Mag.* A **78** 389
[2] Liu C S, Zhu Z G, Xia J C and Sun D Y 2000 *Chin. Phys. Lett.* **17** 34
[3] Daw M S and Baskes M I 1984 *Phys. Rev.* B **29** 6443
[4] Finnis M W and Sinclair J E 1984 *Phil. Mag.* A **50** 45
[5] Ackland G J and Vitek V 1990 *Phys. Rev.* B **41** 10324
[6] Gao F, Bacom D J and Ackland G J 1993 *Phil. Mag.* A **67** 275
[7] Ackland G J 1992 *Phil. Mag.* A **66** 917
[8] Tsjimoto A and Fudoda K 1984 *Metal* **10** 24 (in Japanese)
[9] Hultgren R 1963 *Selected Values of Thermodynamic Properties of Metals and Alloys* (New York: Wiley) p 433–435
[10] Rose J H et al 1984 *Phys. Rev.* B **29** 2963
[11] Mehl M J Osbum J E and Papaconstantopoulos D A 1990 *Phys. Rev.* B **41** 10311
[12] Farkas D 1994 *Modelling Simul. Mater. Sci. Eng.* **2** 975
[13] Brossmans U et al 1994 *Phys. Rev.* B **49** 6457